

Original Article

Interleukin-17 promotes metastasis in an immunocompetent orthotopic mouse model of prostate cancer

David Cunningham¹, Qiuyang Zhang¹, Sen Liu¹, Keshab R Parajuli¹, Qiang Nie^{1,3}, Lin Ma^{1,4}, Allen Zhang¹, Zhenbang Chen⁵, Zongbing You^{1,2,6,7,8}

Departments of ¹Structural and Cellular Biology, ²Orthopedic Surgery, Tulane University, New Orleans 70112, Louisiana; ³Lung Cancer Research Institute and Cancer Center, Guangdong General Hospital, Guangzhou, Guangdong Province, China; ⁴Department of Thoracic Surgery, West China Hospital, Sichuan University, Chengdu, Sichuan Province, China; ⁵Department of Biochemistry and Cancer Biology, School of Medicine, Meharry Medical College, Nashville, Tennessee; ⁶Tulane Cancer Center and Louisiana Cancer Research Consortium, New Orleans, Louisiana; Tulane Centers for ⁷Stem Cell Research and Regenerative Medicine, ⁸Agging, Tulane University, New Orleans, Louisiana

Received June 5, 2018; Accepted June 7, 2018; Epub June 15, 2018; Published June 25, 2018

Abstract: Metastasis of prostate cancer causes substantial morbidity and mortality. The role of chronic inflammatory factors in promoting the development of prostate cancer metastasis remains unexamined due to a lack of immunocompetent animal models. Here we report an orthotopic mouse allograft model of prostate cancer that was used to assess interleukin-17's role in prostate cancer metastasis. A luciferase gene was stably introduced into a mouse prostate cancer cell line MPC3, named as MPC3-luc. MPC3-luc cells were mixed with Matrigel™ and inoculated into C57BL/6 mouse prostates, with recombinant mouse interleukin-17 (IL-17) (treatment group) or without IL-17 (control group). Bioluminescent imaging was used to track the growth and metastasis of prostate cancer metastasis. Immunohistochemistry was performed to confirm metastasis. Mice in the IL-17 treatment group had significantly higher incidence of metastasis than mice in the control group. However, there was no detectable difference in primary prostate tumor growth. Metastases were confirmed as originating from prostate cancer through staining for luciferase protein expression. Our findings suggest that interleukin-17 promotes prostate cancer metastasis in an orthotopic mouse allograft model.

Keywords: Prostate cancer, metastasis, interleukin-17, orthotopic mouse model, MPC3

Introduction

Prostate cancer (PCa) bone metastasis is a substantial public health burden, killing an estimated 29,430 American men in 2018 alone [1]. Despite the high incidence of bone metastasis in lethal cases in humans [2], animal models of spontaneous PCa bone metastasis remain underdeveloped, particularly in the case of immunocompetent mice [3]. The currently favored genetic model for PCa tumorigenesis is the prostate-specific *Pten*^{-/-} mouse and Hi-Myc mouse [4, 5]. However, metastasis in these models is not commonly seen. Similarly, the prostate-specific *Pten*^{-/-}; *p53*^{-/-} double knockout mouse model did not show evident metastasis [6]. However, subsequent

triple knockout mouse models showed an increasing propensity to develop bone metastatic diseases, such as *Pten*^{-/-}; *p53*^{-/-}; *Smad4*^{-/-} model with 3/24 mice showing bone metastases and *Pten*^{-/-}; *p53*^{-/-}; *Rb1*^{-/-} model with 1/4 mice showing bone metastases [7, 8].

In addition to exploring the genetics of cancer, recent advances in the field of cancer treatment have relied on the development of immunotherapy [9]. This indicates a paradigm shift in the way that cancer is viewed, not solely as a genetic or epigenetic disease but as a disease that has important interactions with the immune system. For the studies of immunotherapy, an immunocompetent mouse model of prostate cancer is desired, particularly one

with metastasis to mimic the advanced stage of human prostate cancer that demands immunotherapy. However, such animal models are rare to find.

The aims of the present study were to establish an orthotopic model of prostate cancer in immunocompetent mice and to test the effects of interleukin-17 (IL-17) on primary tumor growth and metastasis. We have previously demonstrated that IL-17 promotes the development of hormone naïve and castration-resistant primary PCa in *Pten*^{-/-} mouse models [10-12]. Here we report that an orthotopic mouse model was established using mouse prostate cancer MPC3 cell line and that IL-17 promoted metastasis in this mouse model of prostate cancer.

Methods and materials

Cell culture

MPC3 cell line was established in the lab of Dr. Zhenbang Chen (Meharry Medical College, Nashville, TN) from *Pten*^{-/-}; *p53*^{-/-} double knock-out mouse prostate cancer [6, 13]. Cells were maintained in DMEM (Caisson Laboratories, Inc., Smithfield, UT) supplemented with 5% FBS (Gemini Bio-Products, West Sacramento, CA) and 1% penicillin streptomycin cocktail (Mediatech, Inc., Manassas, VA). MPC3 cells were transfected with a firefly luciferase construct, a gift from Scott Lowe (plasmid # 18782, Addgene, Cambridge, MA). Transfection was conducted using a Neon Transfection system (Thermo Fisher Scientific, Waltham, MA). Cells were electroporated twice at 1200 volts for 20 milliseconds or once at 1400 volts for 30 milliseconds. Cells were incubated for approximately 60 hours, and then hygromycin (Invitrogen, Carlsbad, CA) was added to the media at an initial concentration of 50 µg/ml. After colonies were established at 5-6 days post transfection, hygromycin concentration was increased by 50 µg/ml every 2-3 days for the rest of the 14-day selection period to a final concentration of 200 µg/ml. The cells were named as MPC3-luc cells after luciferase expression was confirmed with bioluminescent imaging.

Orthotopic cancer cell inoculation

All animal studies were conducted with approval of Institutional Animal Care and Use Committee (IACUC) at Tulane University. Nine to

thirteen weeks old C57BL/6 male mice were obtained from Jackson Laboratory (Bar Harbor, ME) or from in-house breeding. Cells were grown to near confluence on the day of surgery. 5×10⁵ MPC3-luc cells were resuspended in 9 µL of Matrigel™, either with 1 µL 1% bovine serum albumin (BSA) (Control group) or with 1 µL 1% BSA buffer containing 100 ng recombinant mouse IL-17 (rmIL-17; catalogue number 421-ME, R&D Systems, Minneapolis, MN) (Treatment group). Mice were randomized into control or treatment groups by flipping a coin prior to surgery. Mice in the control and treatment groups were operated on in an alternating fashion to avoid bias due to differences in cell viability over the course of the operation because the cells were kept on ice. Mice were initially anesthetized with 3% isoflurane at an induction chamber flow rate of 0.8 L/min. Mice were then positioned sternal on the surgical table with maintenance of 2-2.5% isoflurane through a nosecone. Mice received buprenorphine at a dose of 0.1 mg/kg body weight via intraperitoneal administration. The lower abdominal area was shaved with an electric trimmer and sterilized with 70% ethanol and then betadine solution. A 1-cm incision was cut in the midline of the lower abdomen to expose the abdominal cavity. The bladder was then identified through the surgical window and pulled out of the abdominal cavity to expose the ventral prostate (VP). A 50-µL Hamilton syringe attached to a 26S gauge needle was then used to take up 10 µL of Matrigel™ containing MPC3-luc cells with or without IL-17. The syringe was placed above the head of the mouse to allow for a rostral approach of the needle along the plane of the ventral surface of the body. The needlepoint was inserted just below where the bladder coalesced into the urethra, advancing only as far as the VP. The 10 µL of cell mixture was then administered at a slow rate of approximately 10 µL/min. After injection, the abdominal and skin wound was sutured separately with 5/0 chromic gut suture (CP Medical, Norcross, GA, USA). The animal was then positioned sternal in a cage for 10-15 minutes until becoming conscious.

In vivo bioluminescent imaging

Starting one-week post-surgery, primary tumor growth was assessed using IVIS Lumina XRMS *In Vivo* Imaging System (PerkinElmer, Waltham, MA). Prior to imaging, the instrument was set

to collect a minimum of 20,000 photon counts on the auto settings. Imaging parameters were prioritized as exposure time, binning, and *f* stop. D-luciferin potassium salt (catalogue #MB102, Syd Labs Inc., Natick, MA) was resuspended in phosphate-buffered saline (PBS) to a final concentration of 20 mg/ml. Mice were dosed with 200 μ L luciferin substrate intraperitoneally and waited for 10 minutes to allow for distribution of substrate prior to image acquisition. Animals were anaesthetized with 3% isoflurane with a 1 L/min induction chamber flow rate and maintained at 2% isoflurane at a 0.5 L/min imaging chamber flow rate. After the completion of imaging, mice were replaced in the cage in a sternal position and observed for 10-15 minutes until becoming conscious. Endpoint was determined in consulting with a veterinarian, including the following criteria: palpable tumor in the lower abdomen > 1.5 cm in diameter, inability to eat or drink, inability to ambulate (i.e. when animal failed to move when approached), inability to pass urine, or loss of 15% body weight during the course of weekly weighing. If an animal met three out of the five criteria, it would be euthanized for endpoint analysis. Prior to euthanasia, *in vivo* imaging was performed as described above. Immediately after imaging, the animal was given another dose of D-luciferin and euthanasia was accomplished with CO₂ asphyxia and subsequent cervical dislocation. The animal was weighed intact. The entire genitourinary (GU) bloc was dissected out of the carcass, weighed, and imaged in a Petri dish filled with PBS, adjacent to the carcass. The carcass without GU bloc was imaged again from both ventral and dorsal views for additional luciferase signals that were indicative of metastases. Putative metastatic sites were dissected out and imaged to confirm the tissue origin of luciferase signals, in comparison to the imaging of the carcass. The GU bloc and isolated tissues were fixed in 4% paraformaldehyde overnight at 4°C and subsequently placed in 70% ethanol.

Immunohistochemistry

The fixed tissues were serially dehydrated in increasing concentrations of ethanol and cleared in xylene as previously described.¹⁰ Sectioning for both histopathology and immunohistochemistry (IHC) was accomplished by cutting 4- μ m serial sections. Every fifth section was placed onto a different slide for IHC stain-

ing for luciferase protein and every tenth section was used for histopathological analysis. This accounted for a total of at least 32 consecutive sections from each tissue. Slides were deparaffinized in xylene and rehydrated through serially decreasing concentrations of ethanol. Slides were washed extensively with double distilled H₂O and antigen retrieval was performed by submerging the slides in 0.01 M ethylenediaminetetraacetic acid (EDTA) and boiling for 3 minutes in a water bath, followed by a 20 minute cool down to room temperature. Endogenous peroxidase activity was quenched with 3% H₂O₂. Slides were then blocked in horse serum provided in Vectastain[®] avidin-biotin complex (ABC)-horseradish peroxidase (HRP) kits (mouse kit catalogue number PK-6102, rabbit kit catalogue number PK-6101, Vector Laboratories, Burlingame, CA). Slides were then probed with the following antibodies diluted in normal serum supplied in the kits: mouse anti-luciferase (1:250 dilution, catalogue number NB600-307SS, Novus Biologicals, Littleton, CO), mouse anti-metastasis associated 1 (MTA1) (1:250 dilution, catalogue number sc-373765, Santa Cruz Biotechnology, Dallas, TX), goat anti-MMP7 (1:250 dilution, catalogue number AF2967, R&D Systems, Minneapolis, MN), and rabbit anti-Snail (1:250 dilution, catalogue number 3879, Cell Signaling Technology, Danvers, MA). Primary antibodies were incubated at 4°C overnight. Then, slides were washed and incubated with species-specific secondary antibodies. Slides were probed with ABC reagent with subsequent color development using 3, 3'-diaminobenzidine (DAB) (Vector Laboratories, Burlingame, CA). Hematoxylin was used as a counterstain. Slides were then dehydrated through serially increasing concentrations of ethanol, cleared with xylene, and sealed with Permount[®] mounting medium (catalogue SP15-500, Fisher Scientific, Waltham, MA).

Statistical analysis

Figures were generated using RStudio [RStudio Team (2015), RStudio: Integrated Development for R. RStudio, Inc., Boston, MA URL <http://www.rstudio.com/>] and Microsoft Excel[®]. Statistical analysis was performed using a two-tailed Student's *t*-test with $\alpha < 0.05$ as the threshold for significance unless otherwise noted using Graphpad[®] QuickCals (<https://www.graphpad.com/quickcalcs/>) and the Cancer Research and Biostatistics tool ([116](https://</p></div><div data-bbox=)

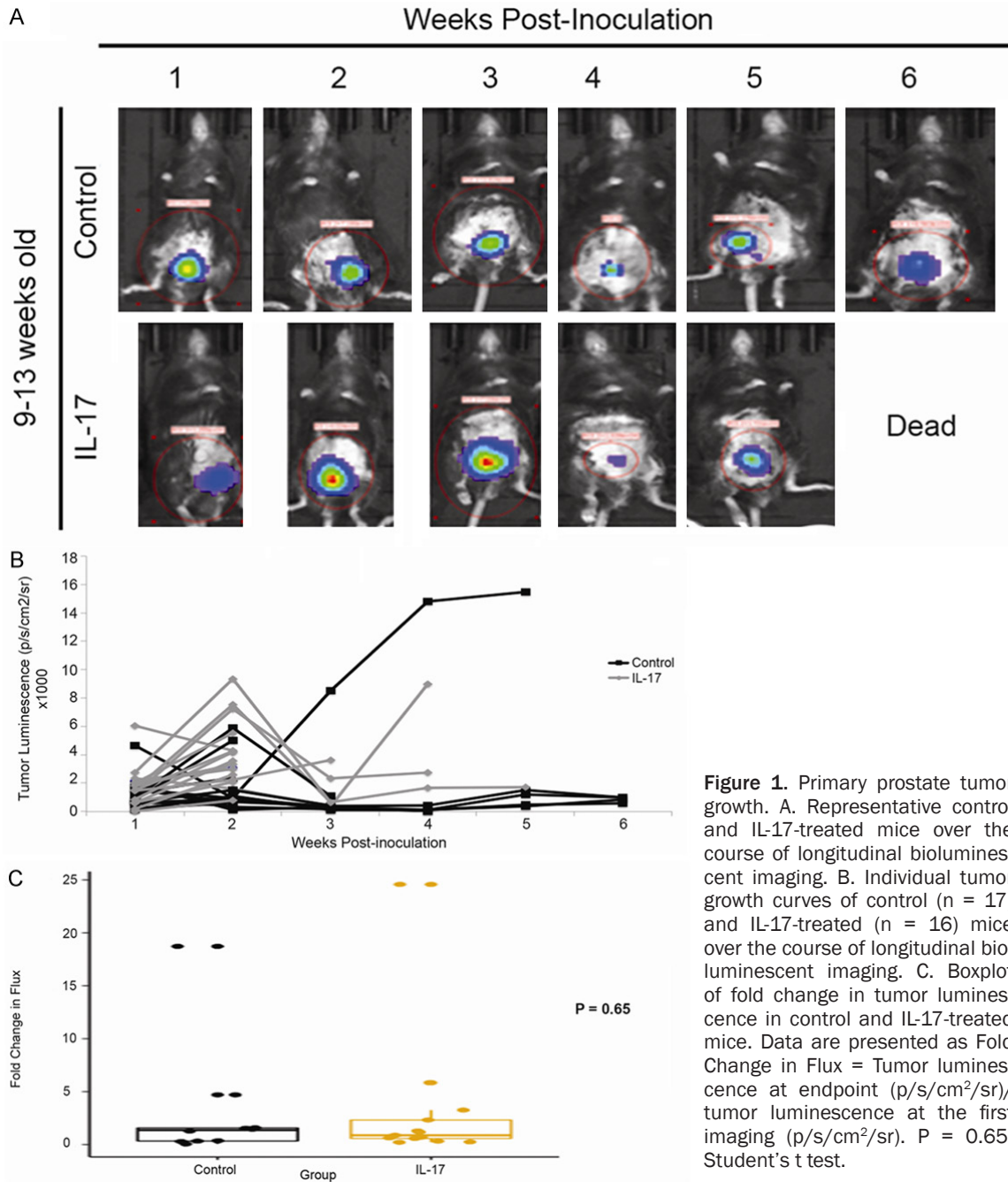


Figure 1. Primary prostate tumor growth. A. Representative control and IL-17-treated mice over the course of longitudinal bioluminescent imaging. B. Individual tumor growth curves of control (n = 17) and IL-17-treated (n = 16) mice over the course of longitudinal bioluminescent imaging. C. Boxplot of fold change in tumor luminescence in control and IL-17-treated mice. Data are presented as Fold Change in Flux = Tumor luminescence at endpoint (p/s/cm²/sr)/tumor luminescence at the first imaging (p/s/cm²/sr). P = 0.65, Student's t test.

stattools.crab.org/Calculators/frequencyTable.htm).

Results

Mice in the treatment group tend to grow larger tumors than mice in the control group

After titrating the proper number of cells to generate tumors in C57BL/6 mice, we found that 5×10⁵ cells inoculated into the VP were able to generate tumors in an initial cohort of mice at a

tumor-take rate of 55% (6 mice in the control group and 5 mice in the treatment group out of n = 10 mice per group; representative mice shown in **Figure 1A**). Using the metastatic rate data from this cohort, we estimated that n = 10/group would give 90% power to detect a 60% difference in the metastatic rates between control and treatment groups. Therefore, we added another cohort of mice (n = 11 mice per group considering the 55% tumor-take rate). This second cohort of mice yielded a tumor-take rate of 100% (11 mice in the control group

IL-17 and cancer metastasis

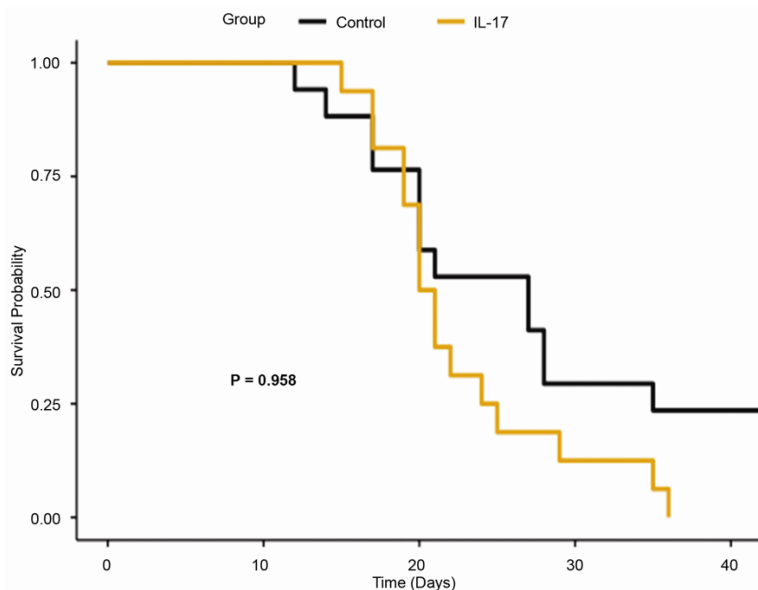


Figure 2. Kaplan-Meier survival analysis of control (n = 17) and IL-17-treated (n = 16) mice. P = 0.096, log-rank test.

and 11 mice in the treatment group). Mice were imaged weekly starting seven days post inoculation. Both cohorts were pooled together for analysis, including n = 17 mice in the control group and n = 16 mice in the treatment group. All mice demonstrated positive luciferase signals upon in vivo bioluminescent imaging and were included in the analysis of primary tumor growth and survival. Despite diligent daily observation, 4 mice in the control group and 2 mice in the treatment group died unexpectedly, thus it was not possible to perform in vivo bioluminescent imaging at the endpoint. These 6 mice were excluded from analysis of metastases, that is, only n = 13 mice in the control group and n = 14 mice in the treatment group were included in analysis of metastases. Individual tumor growth curves are presented in **Figure 1B**. Considering the large variations that became apparent when averaging the two groups' weekly imaging datasets, we used the fold-change in luminescence flux as a way to control for the week-to-week variations and unequal initial luminescence flux. This fold-change was calculated using the endpoint luminescence flux divided by the initial luminescence flux. As depicted in **Figure 1C**, the treatment group appeared to have a larger average fold-change than the control group, although this difference was not statistically significant. Survival probability is an important indicator of cancer aggressiveness. Kaplan-Meier curves derived from survival data showed

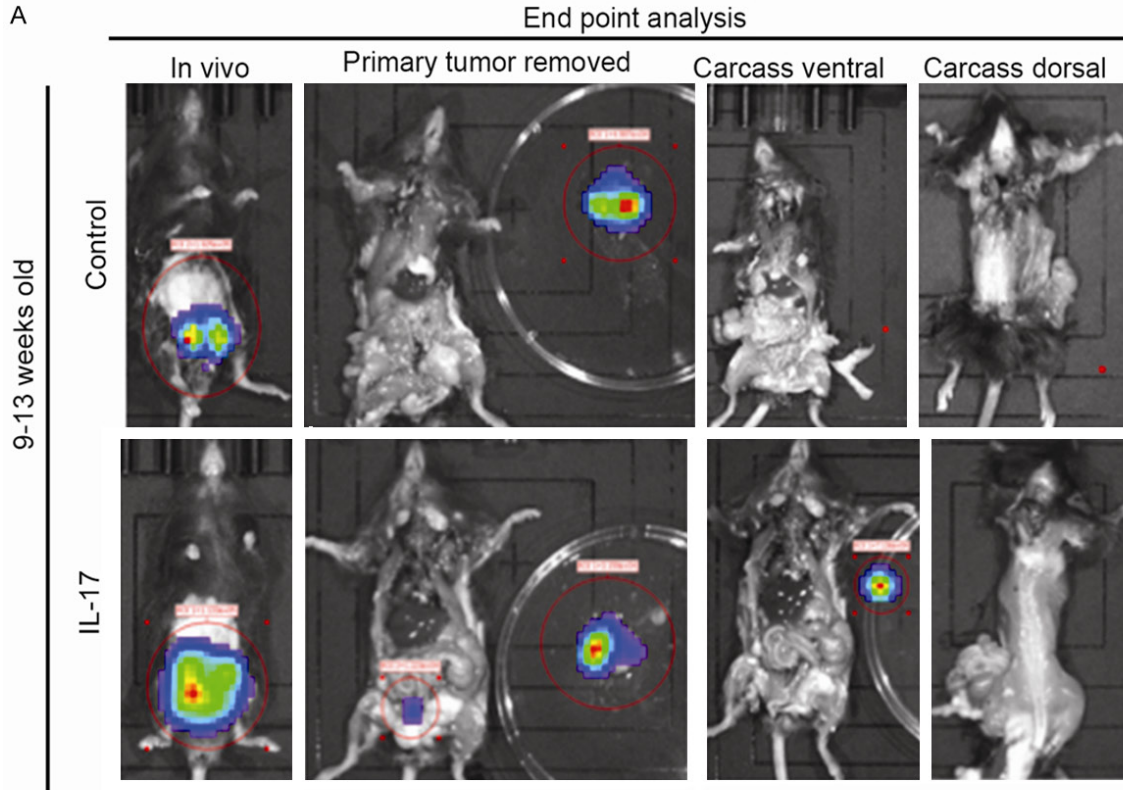
that the treatment group had shorter survival time than the control group, but the difference was not statistically significant (**Figure 2**).

Mice in the treatment group had more metastases than mice in the control group

The primary focus of this study was the comparison of metastases between the control and treatment groups. As shown in **Figure 3**, representative control and treatment animals were depicted in panel A, in which only the treatment mice showed luminescent signals after the primary tumors were removed, indicating existence of metastatic loci. The tissue was iso-

lated and again showed positive luminescent signals. The overall metastatic rates were tabulated in panel B, which showed that 5 mice from the treatment group had metastatic tumors (4 in the pelvic lymph nodes and 1 in the retro-hepatic space). Both Pearson's test and Chi-squared test showed p values < 0.05. These metastatic tumors were subjected to IHC staining of luciferase protein and showed positive staining (**Figure 3C, 3D**), indicating that the metastatic tumors were derived from MPC3-luc cells. It should be noted that due to the sensitivity of the IVIS instrument, several dozen to a few hundred cells in a metastatic tissue would be able to be detected by bioluminescent imaging as shown in the lymph node (**Figure 3C, 3D**).

With the five metastatic tumors confirmed as originating from the prostate tumors, we then looked at several genes previously established as playing a role in epithelial-to-mesenchymal transition (EMT) of spontaneous PCa mouse models [11, 12]. As shown in **Figure 4A**, metastatic tumor cells presented with large nuclei with atypia. Tumor cells were distinguished from stromal and other functional cells of the lymph node by showing nuclear atypia with prominent nucleoli, increased nuclear size, and reduced cytoplasm/nuclear ratio. Both matrix metalloproteinase 7 (MMP7) and Snail were detected in metastatic tumor cells (**Figure 4B, 4D**). On the other hand, metastasis associated



B

Group	Positive for Metastasis (Any location)	Negative for Metastasis
Control	0	13
IL-17*	5	9

* Pearson's test $p = 0.0407$
Chi squared test $p = 0.017$

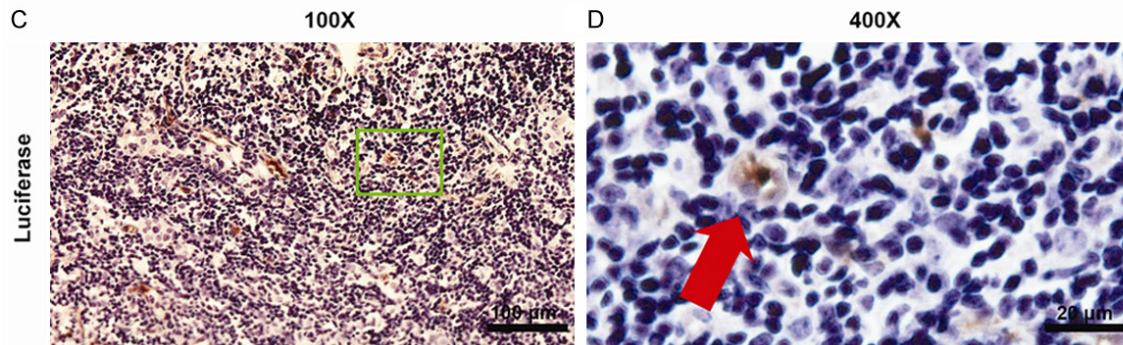


Figure 3. Analysis of metastasis. (A) Animals were imaged immediately prior to euthanasia to confirm primary tumor luminescence *in vivo*, then imaged subsequent to euthanasia to scan for signals outside of the primary tumor after the primary tumor was removed. If any metastatic sites were revealed, the metastatic tissues were dissected out and scanned with the carcass from ventral and dorsal views. The representative IL-17-treated mouse shows signals from a pelvic lymph node. (B) Tabulation of metastatic rates between control and IL-17-treated animals after meeting criteria for endpoint analysis. (C) Representative IHC staining of luciferase protein in a lymph node metastasis; magnification, 100x; scale bar, 100 μ m. (D) High-power view of the region in the green box of (C); red arrow indicates cancer cells with positive luciferase staining in the lymph node; magnification, 400x; scale bar, 20 μ m.

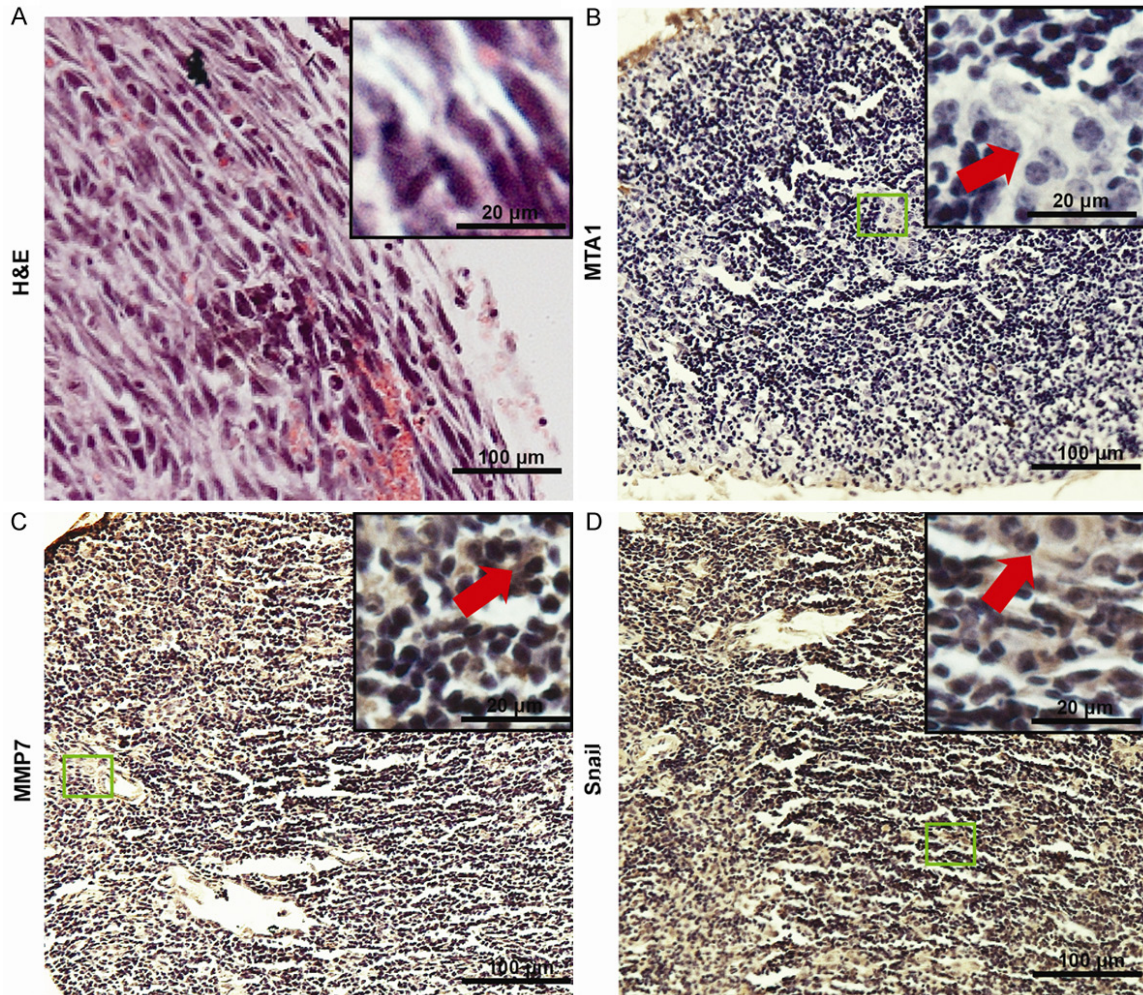


Figure 4. Immunohistochemical staining of markers linked to metastasis. A. Representative hematoxylin and eosin (H&E) staining of a lymph node with metastasis. B. Representative IHC staining for MMP7; red arrow in the inset indicates cells stained positive for MMP7. C. Representative IHC staining for MTA1; red arrow in the inset indicates cells stained negative for MTA1. D. Representative IHC staining for Snail; red arrow in the inset indicates cells stained positive for Snail. Magnification, 100x; scale bar: 100 µm. Magnification of the inset, 400x; scale bar: 20 µm.

gene 1 (MTA1) expression was weak or absent from the tumor cells (**Figure 4C**).

Discussion

Our previous studies have demonstrated that IL-17 promotes the development of hormone-naïve and castration-resistant prostate cancer. IL-17 induces important changes that allow for metastasis, such as degradation of glandular basement membrane, angiogenesis, and EMT [10-12]. This study shows that co-inoculation of recombinant IL-17 and cancer cells promote metastasis of orthotopically allografted mouse prostate cancer. Five of 14 mice in the IL-17 treatment group had metastases to the pelvic

lymph nodes (4 mice) and retrohepatic space (1 mouse). In contrast, none of the 13 mice in the control group had any metastasis. We are confident that the lymph node metastases result from the lymphatic drainage of the prostate similar to human prostate cancer metastasis. The single case of retrohepatic metastasis may be due to lymphatic metastasis or exfoliation of tumor cells into the peritoneal cavity. Even if we exclude this case from analysis, we still have a *P* value of 0.041 using Chi-square analysis of 0/13 (control group) versus 4/14 (treatment group). Therefore, we are confident that IL-17 promotes lymphatic metastasis of prostate cancer in this animal model.

However, we did not see significant differences in primary tumor growth between the control and IL-17 treatment groups. There are several possible reasons that may account for this. First, the large variations in tumor sizes may arise from the unequal inoculation of tumor cells due to the adhesive nature of Matrigel™. Secondly, bioluminescent imaging might be affected by variations in hair removal from week to week. Skin and fur pigmentation has been shown to be a substantial source of signal attenuation in C57BL/6 mice, so minor differences in depilation efficiency is a contributing factor [14]. Thirdly, prostate tumors in this model were rather large, often times growing to 2 cm in diameter with areas of highly necrotic tissues (data not shown). It is possible that, due to luciferase's properties as a marker of viability, tumors maintained viability and luminescence in their invasive fronts while leaving areas of non-luminescent necrotic tissues in its wake. This could account for some of the variations seen in tumors that didn't grow as consistently on a week-to-week basis. Last, the half-life of IL-17 is about minutes to hours and is difficult to detect in serum and bodily fluids [15]. The half-life of IL-17 inoculated in Matrigel™ is unknown, although hypothetically it could extend IL-17's presence in the tumor. We speculate that IL-17 could stimulate some tumor cells to initiate invasion, migration, and metastasis, while it could not stimulate primary tumor growth due to lack of long-term effects once IL-17 is used up or degraded.

One weakness of this study is that despite the significantly different rates of metastasis seen between control and IL-17 treatment groups, none of the metastases was detected in typical human PCa metastatic sites such as the bone. It is still not clear why rodent prostate cancer does not metastasize to the bone. Further studies are needed to create a mouse model of prostate cancer with bone metastasis. Another weakness is that we presented few mechanisms about how the allografted prostate cancer metastasized to the lymph nodes. We found that the metastatic tumors expressed MMP7 that might facilitate tumor invasion. IL-17 is also known to be an angiogenic factor in prostate tumors, which might promote cancer cell intravasation into newly formed blood vessels [11]. We found that the metastatic tumors expressed Snail, a marker of EMT. The presence of Snail at an appreciably high level

indicates that EMT may play a role in the metastasis.

The main novelty of this study, apart from the significance of the metastasis data, is the model in which this study was conducted. The burgeoning field of immuno-oncology and along with it the increasing possibilities of effective immunotherapies are an exciting development in cancer research and treatment. There is therefore a need for models that allow for the preclinical study of the adaptive immune response. To our best knowledge, this is the first study that conclusively shows that MPC3 cells are able to grow in immunocompetent C57BL/6 mice, which makes it one of the few alternatives to the TRAMP derived lines. While TRAMP-C1 cells have been shown to be a model of neuroendocrine prostate cancer, MPC3 cell line can be considered a faithful recapitulation of mouse prostate adenocarcinoma, originally isolated from a genetically engineered mouse that faithfully models primary tumor growth [14, 16]. Ideally, this model will allow for the implementation of immunological studies and the development of immunotherapies that will be able to target and reduce metastatic growth, incidence, and tumor progression. As MPC3 cells were derived from a mixed background mouse whose prostate tumors did not demonstrate any degree of metastasis even after two years of follow up, one possible way to improve this model would be to serially passage MPC3-Luciferase cells through C57BL/6 mice, thus enriching cells more compatible with C57BL/6 background.

Conclusions

IL-17 had no discernible effect on primary tumor growth in this model. Metastatic incidence was higher in the IL-17 treatment group, suggesting that IL-17 may play a role in promoting PCa metastasis in this mouse allograft model.

Acknowledgements

The authors would like to acknowledge Dr. Muralidharan Anbalagan (Tulane University) for material and technical assistance in generating the luciferase positive cell line. This work is partially supported by National Institutes of Health (R01CA174714), Department of Defense (W81XWH-14-1-0050, W81XWH-14-1-0149, and W81XWH-15-1-0444), the Transformative

Experiment Fund of Tulane Cancer Center (TCC), and Louisiana Cancer Research Consortium (LCRC) Fund. The content of this article is solely the responsibility of the authors and does not necessarily represent the official views of the National Institutes of Health or the Department of Defense.

Disclosure of conflict of interest

None.

Address correspondence to: Zongbing You, Department of Structural and Cellular Biology, Tulane University School of Medicine, 1430 Tulane Avenue mailbox 8649, New Orleans 70112, Louisiana. Tel: 504-988-0467; Fax: 504-988-1687; E-mail: zyou@tulane.edu

References

- [1] Cancer Statistics Center 2018. American Cancer Society website. <https://cancerstatistics-center.cancer.org/#/> Accessed March 7, 2018.
- [2] Sartor O, Reid RH, Hoskin PJ, Quick DP, Eil PJ, Coleman RE, Kotler JA, Freeman LM, Olivier P; Quadramet 424Sm10/11 Study Group. Samarium-153-Lexidronam complex for treatment of painful bone metastases in hormone-refractory prostate cancer. *Urology* 2004; 63: 940-945.
- [3] Cunningham D, You Z. In vitro and in vivo model systems used in prostate cancer research. *J Biol Methods* 2015; 2.
- [4] Wang S, Gao J, Lei Q, Rozengurt N, Pritchard C, Jiao J, Thomas GV, Li G, Roy-Burman P, Nelson PS, Liu X, Wu H. Prostate-specific deletion of the murine Pten tumor suppressor gene leads to metastatic prostate cancer. *Cancer Cell* 2003; 4: 209-221.
- [5] Ellwood-Yen K, Graeber TG, Wongvipat J, Iruela-Arispe ML, Zhang J, Matusik R, Thomas GV, Sawyers CL. Myc-driven murine prostate cancer shares molecular features with human prostate tumors. *Cancer Cell* 2003; 4: 223-38.
- [6] Chen Z, Trotman LC, Shaffer D, Lin HK, Dotan ZA, Niki M, Koutcher JA, Scher HI, Ludwig T, Gerald W, Cordon-Cardo C, Pandolfi PP. Crucial role of p53-dependent cellular senescence in suppression of Pten-deficient tumorigenesis. *Nature* 2005; 436: 725-730.
- [7] Ding Z, Wu CJ, Jaskelioff M, Ivanova E, Kost-Alimova M, Protopopov A, Chu GC, Wang G, Lu X, Labrot ES, Hu J, Wang W, Xiao Y, Zhang H, Zhang J, Zhang J, Gan B, Perry SR, Jiang S, Li L, Horner JW, Wang YA, Chin L, DePinho RA. Telomerase reactivation following telomere dysfunction yields murine prostate tumors with bone metastases. *Cell* 2012; 148: 896-907.
- [8] Ku SY, Rosario S, Wang Y, Mu P, Seshadri M, Goodrich ZW, Goodrich MM, Labbé DP, Gomez EC, Wang J, Long HW, Xu B, Brown M, Loda M, Sawyers CL, Ellis L, Goodrich DW. Rb1 and Trp53 cooperate to suppress prostate cancer lineage plasticity, metastasis, and antiandrogen resistance. *Science* 2017; 355: 78-83.
- [9] Kantoff PW, Higano CS, Shore ND, Berger ER, Small EJ, Penson DF, Redfern CH, Ferrari AC, Dreicer R, Sims RB, Xu Y, Frohlich MW, Schellhammer PF; IMPACT Study Investigators. Sipuleucel-T immunotherapy for castration-resistant prostate cancer. *N Engl J Med* 2010; 363: 411-422.
- [10] Zhang Q, Liu S, Xiong Z, Wang AR, Myers L, Melamed J, Tang WW, You Z. Interleukin-17 promotes development of castration-resistant prostate cancer potentially through creating an immunotolerant and pro-angiogenic tumor microenvironment. *Prostate* 2014; 74: 869-879.
- [11] Zhang Q, Liu S, Parajuli KR, Zhang W, Zhang K, Mo Z, Liu J, Chen Z, Yang S, Wang AR, Myers L, You Z. Interleukin-17 promotes prostate cancer via MMP7-induced epithelial-to-mesenchymal transition. *Oncogene* 2016; 36: 867-899.
- [12] Zhang Q, Liu S, Ge D, Zhang Q, Xue Y, Xiong Z, Abdel-Mageed AB, Myers L, Hill SM, Rowan BG, Sartor O, Melamed J, Chen Z, You Z. Interleukin-17 promotes formation and growth of prostate adenocarcinoma in mouse models. *Cancer Res* 2012; 72: 2589-2599.
- [13] Gong Y, Lu W, Xie Y, Yang Q, Matusik RJ, Chen Z. Curcumin suppresses the growth and metastasis of prostate cancer cells by downregulation of Skp2. In: You Z, ed. *Prostate Cancer Cells: Detection, Growth and Treatment*. 1st edition. Happaugue, New York: Nova Science Publishers; 2012. pp. 87-102.
- [14] O'Neill K, Lyons SK, Gallagher WM, Curran KM, Byrne AT. Bioluminescent imaging: a critical tool in pre-clinical oncology research. *J Pathol* 2010; 220: 317-27.
- [15] Cowan J, Pandey S, Filion LG, Angel JB, Kumar A, Cameron DW. Comparison of interferon- γ , interleukin (IL)-17- and IL-22-expressing CD4 T cells, IL-22-expressing granulocytes and proinflammatory cytokines during latent and active tuberculosis infection. *Clin Exp Immunol* 2012; 167: 317-329.
- [16] Astigiano S, Puglisi A, Mastracci L, Fais S, Barbieri O. Systemic alkalinisation delays prostate cancer cell progression in TRAMP mice. *J Enzyme Inhib Med Chem* 2017; 32: 363-368.